ACS OMEGA

http://pubs.acs.org/journal/acsodf

Article

Superhydrophilic and Underwater Superoleophobic Cotton Fabric for Oil−Water Separation and Removal of Heavy-Metal Ion

Xiaohong Li, Ying Chen,* Yong Chen,* Dong Chen, Quan Wang, and Yan Wang

Cite This: *ACS Omega* 2022, 7, 30184−30196

Read Online

ACCESS | Metrics & More | Article Recommendations

ABSTRACT: Superhydrophilic and underwater superoleophobic cotton fabric (named CS-CF-PDA, or m-CF) was prepared by modifying the cotton fabric (CF) with dopamine (DA) and chitosan (CS). The oil−water separation and heavy-metal ion (e.g., Cu(II)) adsorption performances of m-CF were investigated, and m-CF was characterized by field emission scanning electron microscopy (FE-SEM), energy-dispersive spectroscopy (EDS), Fourier transform infrared (FT-IR), and thermogravimetric analysis (TGA). The results showed that the underwater oil contact angle (UWOCA) of m-CF was more than 156°. The m-CF was used to treat artificial oily wastewater containing Cu(II) under room temperature and atmospheric pressure and gravity, by which the separation efficiency, water flux, and Cu(II) removal rate could reach 99%, 17 400 $L \cdot m^{-2} \cdot h^{-1}$, and 89%, respectively. Additionally, in the process of continuous treatment of oily wastewater, the water flux slightly decreased; on the contrary, the Cu(II) removal rate decreased significantly to 67% within 120 s. Cu(II) was one of the reasons for the decrease of water flux. The m-CF of adsorbed Cu(II) could be leached with HCl (0.1 $mol \cdot L^{-1}$) solution, and the Cu(II) desorption rate could reach over 95% within 120 s. After strong acid, strong alkali, high salt, and abrasion treatment, the UWOCAs of m-CF were still higher than 150°. In a word, in terms of oil−water separation, m-CF exhibited good acid, alkali, salt, and abrasion resistances. Also, it is an underwater superoleophobic material involving simple preparation, low cost, and environmental friendliness, which could remove the floating oil and heavy-metal ions from wastewater and has good industrial application prospects.

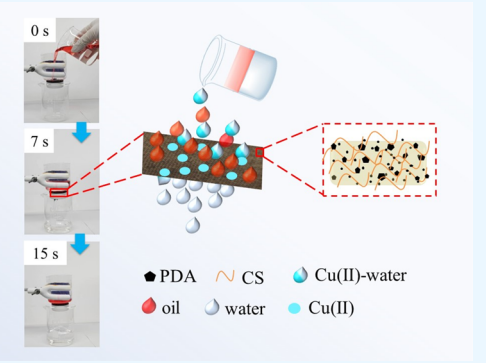

1. INTRODUCTION

With the rapid development of the petroleum and chemical industries, the discharge of oily wastewater and the risk of oil spill accidents increased;[1−3] it was the goal of people's continuous efforts to develop efficient and environmentally friendly methods for treating oily wastewater. So far, many technologies have been reported for the disposal of oily wastewater, including flotation, centrifuges, oil skimmers, membrane separation, etc.[4] The membrane separation method based on a superwetting surface has been attracting extensive attention in the field of oily wastewater treatment because of its simple operation and high separation efficiency.[5−8] Notably, oily wastewater contains other pollutants, such as organic dyes and heavy-metal ions, among which heavy-metal ions are one of the most common and harmful pollutants in water pollution.[9,10] Adsorption is one of the most commonly used methods to remove heavy metals because of its simple operation, easy recycling, and low cost.[9,11−13] A superhydrophilic membrane with functional groups for heavy-metal ion adsorption could simultaneously remove oil and heavy-metal ions from wastewater, which simplifies the purification process of oily wastewater containing heavy-metal ions and reduces the cost of wastewater treatment.[14−20] Wang et al.[14] prepared an organic-inorganic composite membrane by the electrospinning technique modified with 3-[(trimethoxysilyl) propyl]-diethylenetriamine to obtain a superhydrophilic and underwater superhydrophobic membrane. The membrane was used to treat artificial emulsified oily wastewater with the desired concentrations of heavy-metal ions Pb(II), Cr(III), and Ni(II); the water flux could reach 1517 ± 53 $L \cdot m^{-2} \cdot h^{-1}$, and the removal efficiencies of both oil and heavy-metal ions were larger than 99%.

Cotton fabric (CF), which is abundant in nature, easily biodegradable, and environmentally friendly, is widely used as a substrate for the preparation of oil−water separation membranes.[3,8,21] Chitosan (CS) is a natural polymeric alkaline polysaccharide with abundant sources, degradable, and eco-friendly; it contains a large number of functional groups (such as $-NH_2$ and −OH, etc.) that can interact with heavy-metal ions,[9,22,23] resulting in its being widely used to treat heavy-

Received: May 27, 2022
Accepted: August 5, 2022
Published: August 16, 2022

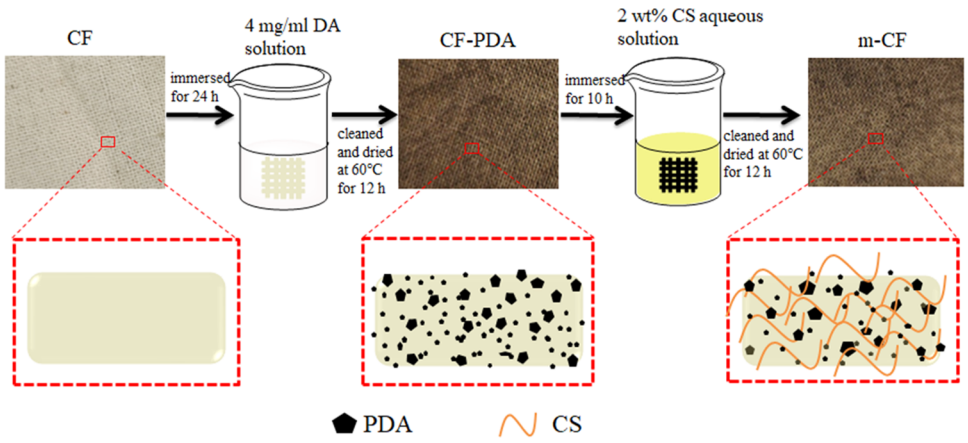

Figure 1. Schematic Representation of the Preparation of m-CF.

metal wastewater by adsorption.[8,11,24] Therefore, environmentally friendly membrane materials for oil−water separation and heavy-metal ion removal can be obtained by using the CS-modified CF.[25] Krishnamoorthi et al.[25] prepared a superhydrophilic CA-CS-CF membrane by using laccase to initiate the oxidation of catechol groups in caffeic acid (CA) to generate reactive quinoids, which were subsequently cross-linked with the amino groups of CS to coat CS on CF. They found that the membrane after multilayer compaction was used to treat artificial emulsified oily wastewater containing heavy-metal ions (Cu(II), Pb(II), and Hg(II)), which yielded good water flux, oil−water separation efficiency, and heavy-metal removal rate.

In general, there are a few reports on superhydrophilic and underwater superhydrophobic cotton fabric materials for simultaneous removal of heavy-metal ions and oils from wastewater.[25] Dopamine is an established mussel-inspired molecule that forms a hydrophilic surface when self-polymerized to form polydopamine (PDA) on various substrates.[25,26] CS can be coated on the substrate by cross-linking the amino group on it with the quinone structure in the polydopamine molecule.[25,27−29] Therefore, we propose to prepare a modified CF by coating the CS on CF with PDA to treat oily wastewater to study its performances of oil−water separation and removal of heavy-metal ions, which can provide technical support for the industrial application of environmentally friendly and low-cost cotton fabric superwetting membranes.

2. EXPERIMENTAL SECTION

2.1. Materials. Chitosan (CS, deacetylation degree ≥ 95%) was purchased from Aladdin industrial Corporation. Dopamine hydrochloride (DA, 98%) was purchased from Sinopharm Chemical Reagent Co., Ltd. Tri-(hydroxymethyl) aminomethane hydrochloride (Tris-HCl, AR) was purchased from Chengdu Aikeda Chemical Reagent Co., Ltd. All of the reagents (hexane, toluene, glacial acetic acid, absolute ethyl alcohol, HCl, NaOH, NaCl, Sudan red III, $CuCl_2{\cdot}2H_2O$ (AR)) were used without further purification. Deionized water was self-made through a laboratory water purifier. The fabric used was commercially available cotton fabric (CF, thickness 0.4 mm).

2.2. Preparation of m-CF. Figure 1 shows the preparation process of the modified CF (named m-CF). The CF was ultrasonically cleaned with ethanol for 20 min and deionized water three times, and then dried in the oven at 60 °C before use. Preparation of modified CF was done according to the literature:[30] 4 $mg{\cdot}mL^{-1}$ dopamine hydrochloride (DA) was dissolved in 100 mL of Tris-HCl buffered aqueous solution (pH 8.5); the cleaned CF was put into the prepared DA buffer solution. Oxidative polymerization of DA generated polydopamine (PDA) after 24 h of reaction with constant shaking and at room temperature, which was deposited on the surface of CF. The obtained hydrophilic modified CF (named CF-PDA) was rinsed several times with deionized water, then dried in vacuum at 60 °C for 6 h. 2 wt % of chitosan (CS) solution was prepared by dissolving CS in 1% glacial acetic acid solution under magnetic stirring condition. The CF-PDA was immersed in CS solution for 10 h, then washed with 0.1% NaOH and a large amount of deionized water, and then dried in vacuum at 60 °C for 6 h to prepare the m-CF.

2.3. Characterization Analysis. The surface morphologies and element mappings of the samples were observed by field emission scanning electron microscopy (FE-SEM, Tescan Mira 3XH) at an accelerating voltage of 3 kV and by energy-dispersive spectroscopy (EDS, Aztec X-MaxN80), respectively. Thermogravimetric analysis (TGA) was performed under air atmosphere with 10 $°C{\cdot}min^{-1}$ heating rate from 25 to 600 °C, and the weight of the samples was about 8−10 mg. Fourier transform infrared (FT-IR) spectrum was recorded to investigate the modified effect and chemical compatibility between pristine CF and modified CF, and the testing wavenumber range was 4000−400 cm^{-1}. Determination of oil in water was done with an infrared spectrophotometry oil measuring instrument (JLBG-126). The wettability of the samples was characterized by a contact angle measuring instrument. The infiltration in air and underwater oil contact angle were measured with 10 μL of water and *n*-hexane, respectively. The time required for the water droplet (10 μL) from just touching the sample surface to spread (i.e., the water contact angle was 0°) was named the water drop infiltration time (WIT).

2.4. Simultaneous Removal of Oil and Cu(II) by m-CF. The separation experiment of 100 mL of artificial oily wastewater containing oil and Cu(II) was carried out using m-CF (effective area was 9.6 cm^2) under gravity and pre-wetted by water prior to use. Toluene (dyed by Sudan Red III) was used as the oil phase (30 mL); deionized water and $CuCl_2$ were used to prepare the water solution, wherein the concentration of Cu(II) was 5 $mg{\cdot}L^{-1}$ (70 mL, pH 5.6). For

https://doi.org/10.1021/acsomega.2c03298
ACS Omega 2022, 7, 30184−30196

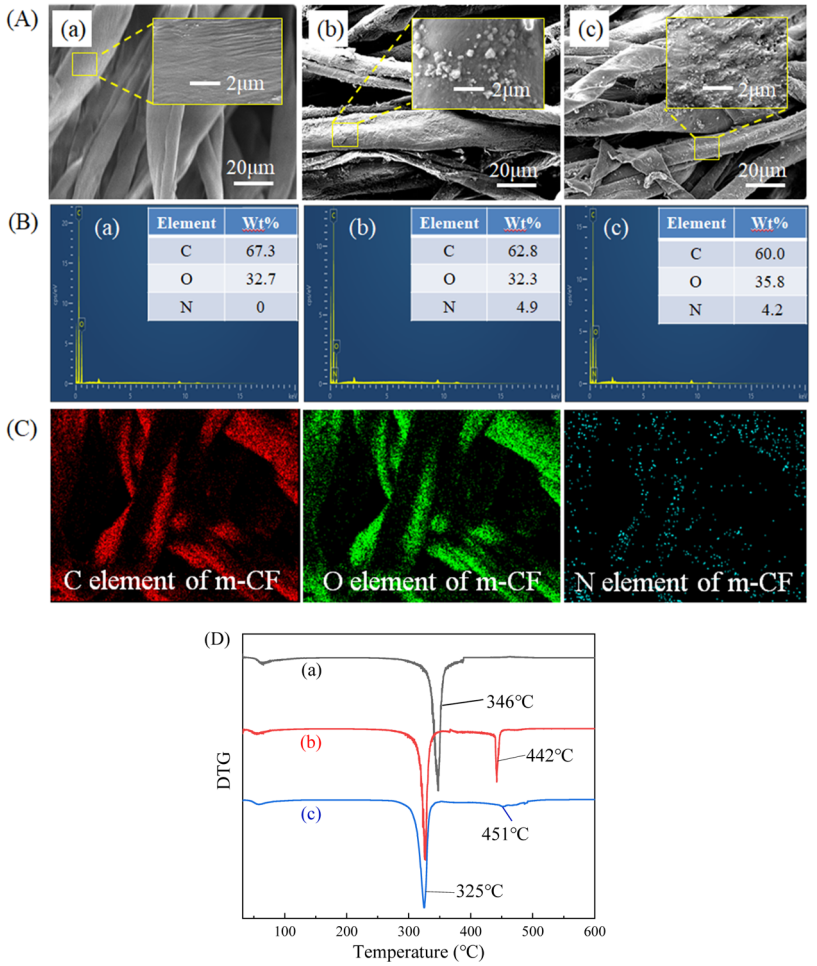

Figure 2. Characterization and analysis of samples by SEM (A), EDS (B), EDS mapping images (C), and DTG (D): (a) CF, (b) CF-PDA, and (c) m-CF.

clearly, the artificial oily wastewater was denoted as "oil−water", and the Cu(II) containing artificial oily wastewater was denoted as "Cu(II)−oil−water". The concentration of Cu(II) was determined via an inductively coupled plasma atomic emission spectrophotometer (ICP-AES). The oil−water separation efficiency and water flux are calculated using eqs (1) and (2), respectively. The Cu(II) removal rate and adsorption capacity are calculated using eqs (3) and (4), respectively.

$$E = \frac{M_1}{M_0} \times 100\% \quad (1)$$

$$F = \frac{V_1}{St} \quad (2)$$

$$R = \frac{C_0 - C}{C_0} \times 100\% \quad (3)$$

$$Q = \frac{(C_0 - C)V}{M} \quad (4)$$

where E and F are the oil−water separation efficiency (%) and water flux ($L \cdot m^{-2} \cdot h^{-1}$), respectively. R and Q are the removal rate (%) and adsorption capacity of Cu(II) (mg/g), respectively. M_0 and M_1 represent the weight of water or water solution in the original mixture and the collected water after separation (g), respectively. S is the effective area of m-CF (m^2), V_1 is the volume of water (L) passing through the m-CF, and t is the permeate time (h). C_0 and C are the initial and final concentrations of copper ions in water (mg/L), respectively; V is the volume (L) and M is the weight of the m-CF (g).

2.5. Chemical Stability of m-CF. To evaluate the chemical stability of m-CF,[30,31] it was immersed in strong acid (HCl solution, 0.5 $mol \cdot L^{-1}$), strong alkali (NaOH solution, 0.5 $mol \cdot L^{-1}$), and high salt solution (NaCl solution, with a concentration of 3.5, 10, and 36%, respectively) for 20 days, washed with deionized water, and dried at 60 °C. The obtained samples were named HCl-m-CF, NaOH-m-CF, $NaCl_{(3.5\%)}$-m-CF, $NaCl_{(10\%)}$-m-CF, and $NaCl_{(36\%)}$-m-CF, respectively. Then, their wettability and the adsorption capacity were investigated.

2.6. Abrasion Treatment of m-CF. The mechanical stability and adsorption capacity of m-CF were evaluated by rubbing on a sandpaper,[32] in which 500# sandpaper served as an abrasion surface, m-CF was placed and moved on the sandpaper under a 200 g weight, and m-CF was dragged back and forth (40 cm as a cycle) in one direction with a speed of 4 $cm \cdot s^{-1}$, and then the wetting behavior was tested after 300 cycles of sandpaper abrasion. The sample was named abrasion-m-CF after abrasion treatment.

https://doi.org/10.1021/acsomega.2c03298
ACS Omega 2022, 7, 30184−30196

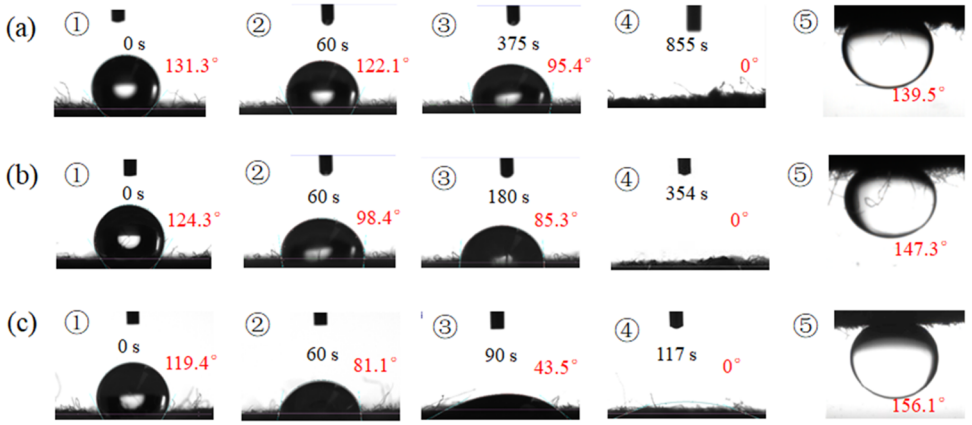

Figure 3. Surface wettability of the samples toward water and oil on the surface of (a) CF, (b) CF-PDA, and (c) m-CF (①−④optical snapshots for the dynamic contact processes of the water droplets; ⑤UWOCA).

3. RESULTS AND DISCUSSION

3.1. Characterizations. The surface morphologies of the samples were investigated by SEM and EDS. According to Figure 2A,B, the surface of CF was smooth.[30] PDA particles with different sizes and irregular shapes were distributed on the surface of CF-PDA, which contained 4.9 wt % of N element. Compared with CF-PDA, the particle size on the surface of m-CF was more unifrom, and the content of N element was slightly reduced (4.2 wt %). DA was oxidized and polymerized on the surface of CF to form PDA particles, and long-chain CS were "wound" around the PDA particles when grafted on the CF-PDA surface, which made the depth of the "gully" formed between PDA particles shallower.[30] The chemical formulas of DA and CS were $C_8H_{11}NO_2$ and $(C_6H_{11}NO_4)_n$, respectively. The content of N in CS was 8.7% by weight, which was slightly less than that of DA (9.2% by weight). Therefore, the N content of CS grafted on CF-PDA was slightly low.

The DTG curves (differential form of TGA) are shown in Figure 2D. The weight loss peak of CF (Figure 2D(a)) at 346 °C can be attributed to the decomposition of the cellulose chain of the cotton fabric.[24,33,34] The weight loss peak of CF-PDA (Figure 2D(b)) appeared at 325 and 442 °C, respectively. Besides, the weight loss was lower than that of CF. The weight loss peak at 442 °C could be attributed to PDA, which may have degraded some substances on the fiber under alkaline environment (pH 8.5), leading to the easy oxidation and decomposition of the fiber and decrease of the weight loss at low temperature. The weight loss peaks of m-CF (Figure 2D(c)) appeared at 325 and 465 °C, respectively. The peak value of high-temperature weight loss increased and its shape widened compared with CF-PDA. The high-temperature peak could be attributed to the decomposition of CS and PDA, and the grafting of CS may also have changed the thermal decomposition performance of PDA, resulting in the increase of the width and peak value of the high-temperature weight loss peak of m-CF.

The above analyses showed that both PDA and CS were successfully coated on CF and the distribution of C, O, and N elements on m-CF was consistent (Figure 2C).

3.2. Wettability of the Sample. For the porous material that is hydrophilic and rich in capillaries, the capillary pressure is one of the main driving forces of water penetration into it. According to the Young−Laplace equation (eq (5)), the smaller the contact angle of water in the inner wall of the capillary (i.e., the stronger the hydrophilicity), the greater the capillary pressure.

$$\Delta p = \frac{2\gamma_{WA}\cos\theta_{WA}}{R} \tag{5}$$

where Δp is the pressure difference between the upper and lower liquid surfaces of the capillary, θ_{WA} is the water contact angle of the water on the capillary wall, R is the capillary radius, and γ_{WA} is the surface tension of water.

The water drop infiltration time (WIT) on porous materials can be calculated by Washburn equation (as shown in eq (6)). Equation (6) shows that the longer the WIT on the porous material, the larger the contact angle of water on the capillary wall, and the weaker the hydrophilicity of the material.

$$\frac{l^2}{t} = \frac{\gamma_{WA}\cos\theta_{WA}}{2\eta}R \tag{6}$$

where t is the infiltration time of the water droplet on porous materials, l is the capillary length, and η is the viscosity of water.

Obviously, the longer the WIT on the porous material, the lesser the capillary force that pushes the water through the membrane.

According to the Wenzel equation (as shown in eq (7)), the surface roughness reduces the water contact angle and enhances the hydrophilicity of the material.

$$\cos\theta'_{WA} = r\cos\theta_{WA} \tag{7}$$

where θ_{WA}' is the water contact angle of the rough surface, and r is the surface roughness factor (i.e., the roughness factor is the ratio of actual surface area to the apparent surface area; r is always larger than 1).

Figure 3 shows the experimental results of wettability of the samples. According to Figure 3, the WIT values of CF, CF-PDA, and m-CF were 855, 354, and 117 s, respectively, and the underwater oil contact angles (UWOCA) were 139.5, 147.3, and 156.1°, respectively. CF was mainly composed of cellulose, which was rich in hydrophilic groups (−OH). The surface or capillary wall of CF was hydrophilic, and the water contact angle was less than 90° ($\theta_{WA} < 90°$). According to the Young−Laplace equation (eq (5)), the capillary force generated on the CF can absorb water into the capillary. DA had polar groups (such as −OH and $-NH_2$) as well as oxidative polymerization on the surface of CF to form PDA particles, making the surface

https://doi.org/10.1021/acsomega.2c03298
ACS Omega 2022, 7, 30184−30196

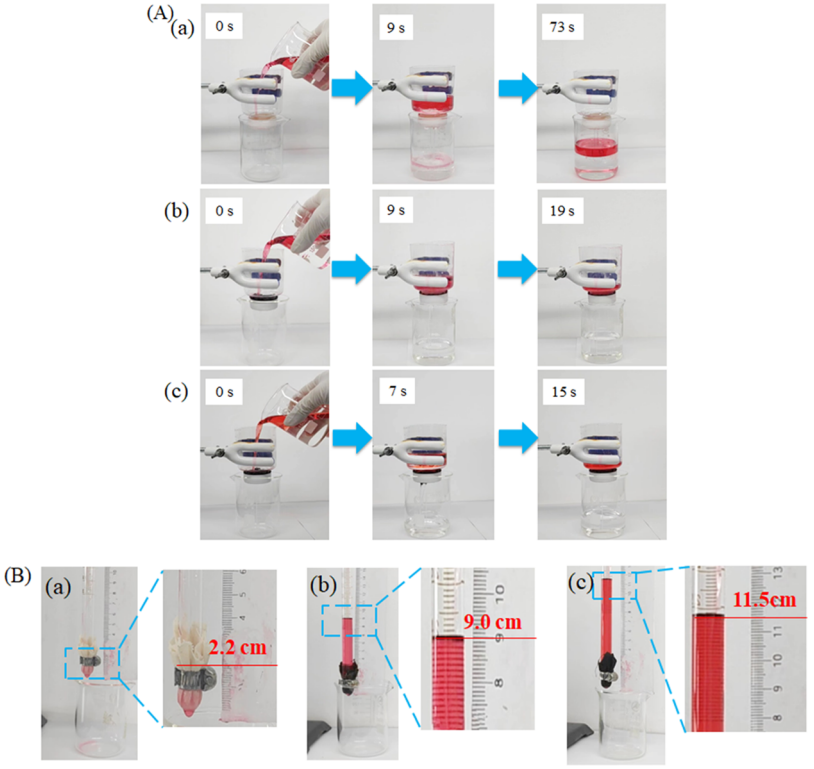

Figure 4. Experimental phenomena of the treatment of Cu(II)−oil−water with the samples at room temperature (A); the height of the oil column of the samples (B): (a) CF, (b) CF-PDA, and (c) m-CF.

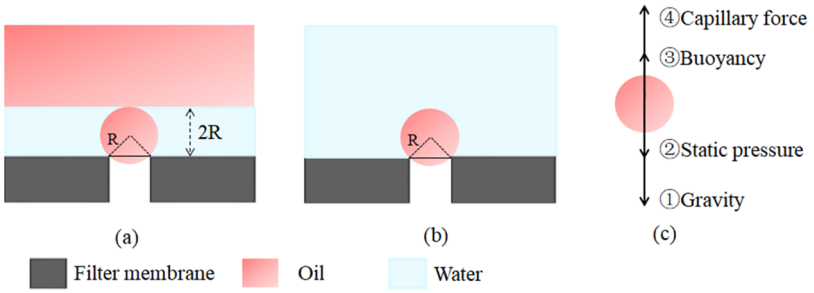

Figure 5. Schematic diagram of forces acting on the oil droplets on the "water-removing" type porous materials (Note: the oil droplets are very small and the static pressure of the water column at 2R height is negligible). (a) Oil above the filter membrane, (b) water above the filter membrane, and (c) forces analysis of the oil droplet.

of the material rough (Figure 2B(b)). Compared with CF, therefore, the hydrophilicity of the CF-PDA surface or capillary inner wall increased and the WIT of the material decreased; at the same time, the UWOCA increased. We knew that the content of non-hydrocarbon elements (O and N) in CS ($(C_6H_{11}NO_4)_n$) was higher than DA ($C_8H_{11}NO_2$), which enhanced the hydrophilicity of m-CF, while UWOCA increased and showed the superoleophobic state (θ_{OWS} > 150°).

3.3. Performance of m-CF Experiments. Figure 4A shows the experimental phenomenon of oil−water separation. It can be seen from the figure that both oil (red) and water can pass through CF; in contrast, for CF-PDA and m-CF, water can completely permeate through, while oil cannot.[30] Among them, it took a shorter time (only 15 s) for water to pass thoroughly through m-CF. Figure 4B shows the photographs of the critical heights of the oil column of CF, CF-PDA, and m-CF, which were 2.2, 9.0, and 11.5 cm, respectively. Besides, the loading of PDA and CS on CF (i.e., m-CF), compared with unmodified CF, brought about a decrease in R and an increase in θ_{OWS}, resulting in the increase in the H_{OC} (see eq 8). Therefore, m-CF had a higher oil repellent ability than CF-PDA.

When using a hydrophilic-oleophobic material for oil−water separation, the combined action of three forces determined whether the oil droplets could permeate through the filter membrane (as shown in Figure 5): (1) The porous material surface is superoleophobic under water; the oil droplets on the surface of the modified CF are subjected to an upward capillary force. (2) If the density of oil is lighter than that of water, it will be subjected to upward net buoyancy. (3) Neglecting the net buoyancy, the oil droplets will permeate through the filter membrane when the capillary force is less than the static pressure of the liquid. According to Young−Laplace equation and hydrostatics equation, we can know the critical liquid height when the oil droplet can pass through the filter membrane (as shown in eqs (8) and (9)); when the actual

https://doi.org/10.1021/acsomega.2c03298
ACS Omega 2022, 7, 30184−30196

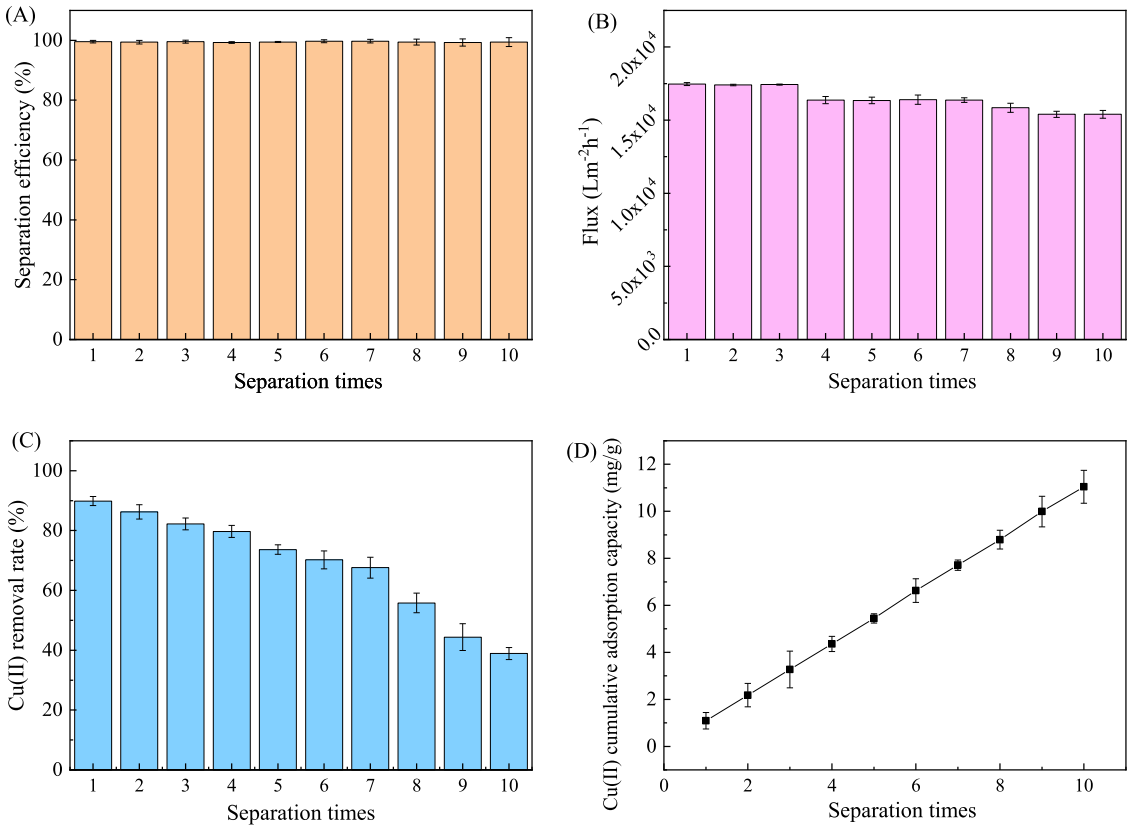

Figure 6. Simultaneous removal of oil and Cu(II) by m-CF at room temperature; oil−water separation efficiency (A), flux (B), Cu(II) removal rate (C), and cumulative adsorption capacity of Cu(II) (D).

liquid height is larger than the critical liquid height, the oil droplet will penetrate the filter membrane.

$$H_{oc} = \frac{2\gamma_{ow}\cos\theta_{ows}}{\rho_0 gR} \quad (8)$$

$$H_{wc} = \frac{2\gamma_{ow}\cos\theta_{ows}}{\rho_w gR} \quad (9)$$

where H_{OC} is the critical height of oil, H_{WC} is the critical height of water, ρ_O and ρ_W are the densities of oil and water, respectively, γ_{ow} is the oil−water interfacial tension, and θ_{OWS} is the contact angle of the underwater oil on the solid surface (i.e., UWOCA).

Commonly if $\rho_O < \rho_W$, then $H_{OC} > H_{WC}$. Therefore, when the total heights of liquid and oil in the oil−water separation equipment are less than H_{WC}, it can ensure that the oil droplets do not pass through the filter membrane and successfully separate oil from water. Obviously, the larger the θ_{OWS}, the higher the H_{WC}, or the smaller the particle size of the oil droplets that can just pass through the filter membrane under certain conditions, the higher the oil−water separation efficiency.

The loading of PDA and CS on CF (i.e., m-CF), compared with unmodified CF, led to a decrease in R and an increase in θ_{OWS}, resulting in the increase in H_{WC}. Therefore, when the oil−water separation conditions are the same, the m-CF material can carry out oil−water separation successfully while CF cannot. These results are consistent with those in Figure 4.

Figure 6 shows the continuous treatment of the solution containing oil and Cu(II) wastewater (i.e., Cu(II)−oil−water), which was divided ten times to investigate the performances of m-CF. As shown in Figure 6A,B, respectively, the E value of m-CF was larger than 99%, which was almost unchanged with the increasing time of the experiments, and the F values of the first time and the tenth time were about 17 400 and 15 400 L·m^{-2}·h^{-1}, respectively, which was decreased by 11%. The R value is shown in Figure 6C, which was 89% in the first experiment and decreased by 57% in the tenth time. Meanwhile, in a similar study by Krishnamoorthi et al.,[25] the water flux, oil−water separation efficiency, and heavy-metal ion removal rate were 50 050 L·m^{-2}·h^{-1}·bar^{-1}, 99, and 99%, respectively. Compared with our study, the reason for the higher water flux and heavy-metal ion removal rate of the membrane may be that it was allowed under pressure and was treated by multilayer compaction. Figure 6D shows that the Cu(II) cumulative adsorption capacity on the membrane after ten times of continuous treatment of wastewater by m-CF (named used-$I_{(10)}$-m-CF) was about 11.0 mg·g^{-1}. The above results indicated that (1) the m-CF had good oil−water separation efficiency and water flux, as well as removed trace amounts of Cu(II) from water solution. (2) With the increasing times of the experiments, the cumulative adsorption capacity of Cu(II) on m-CF increased, while the strength of the adsorption site or non-adsorption site decreased, resulting in the reduction in the removal rate of Cu(II).[35,36] (3) With the increasing times of the experiments, the water flux decreased gradually, while the oil−water separation efficiency remained almost unchanged. What was the reason for the decrease of water flux of the m-CF? Therefore, the used-$I_{(10)}$-m-CF was analyzed by SEM, EDS, FT-IR, and DTG, as shown in Figure 7.

https://doi.org/10.1021/acsomega.2c03298
ACS Omega 2022, 7, 30184−30196

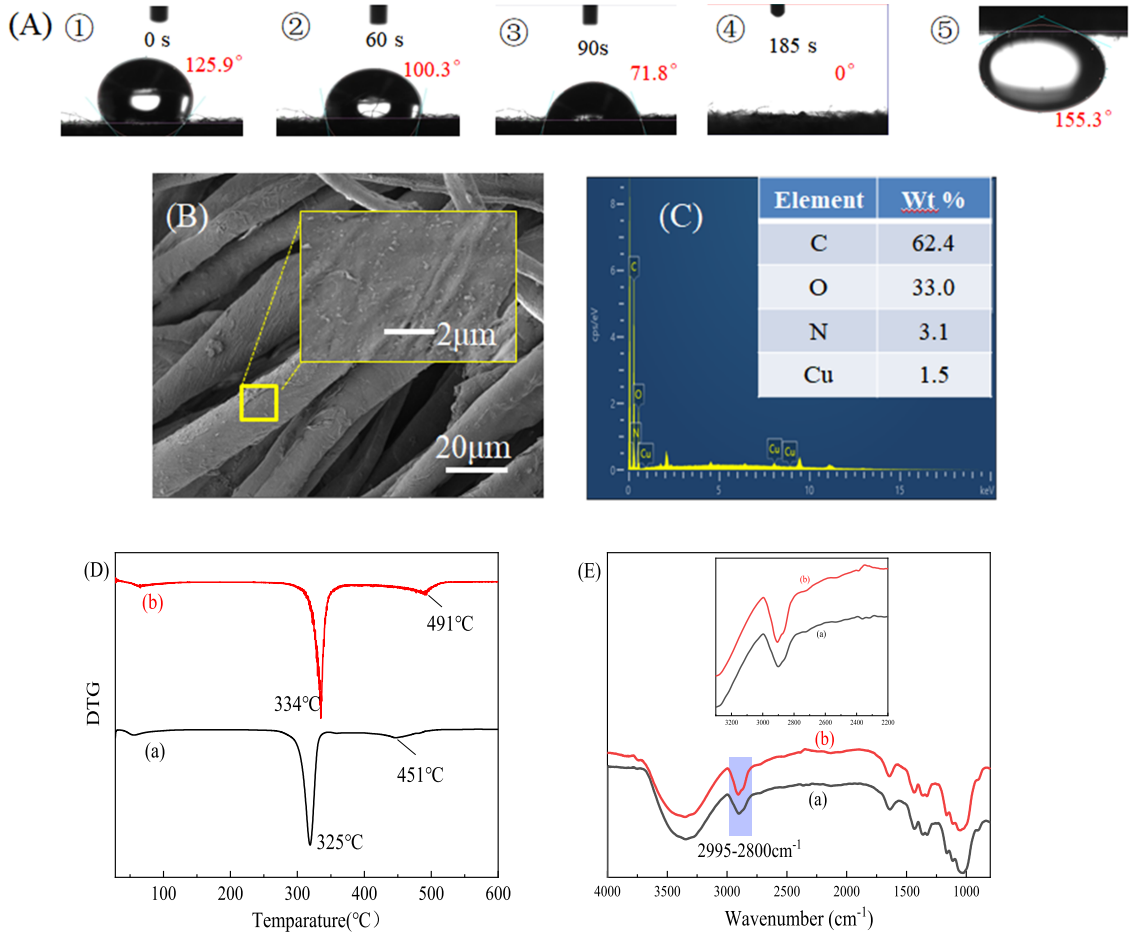

Figure 7. Wettability and characterization analysis of used-$I_{(10)}$-m-CF. Wettability (A) (①–④optical snapshots for the dynamic contact processes of the water droplets,⑤UWOCA), SEM (B), EDS (C), DTG (D), and FT-IR (E): (a) m-CF and (b) used-$I_{(10)}$-m-CF.

As shown in Figure 7A,C, the WIT of used-$I_{(10)}$-m-CF was 185 s and UWOCA was 155.3°. Compared with m-CF, the surface roughness of used-$I_{(10)}$-m-CF decreased slightly and the Cu element appeared with a content of 1.5 wt %, which was close to the result in Figure 6D. The oil was slightly soluble in water (under the conditions of room temperature and atmospheric pressure, the solubility of toluene in water is about 0.5 g·L^{-1}). It may be that when the aqueous phase containing trace amounts of oil permeated m-CF, the oil was absorbed and filled in the "gully" on the surface of the membrane, resulting in the slightly decreased roughness of used-$I_{(10)}$-m-CF.

Figure 7D shows that the two thermal degradation peaks of used-$I_{(10)}$-m-CF were higher than those of m-CF, which were 334 and 491 °C, respectively. It was possible that the adsorption of Cu(II) increased the difficulty of pyrolysis of used-$I_{(10)}$-m-CF.

As shown in Figure 7E, the absorption peak of used-$I_{(10)}$-m-CF at 2995−2800 cm^{-1} (methyl and methylene) was slightly stronger than that of m-CF. The methyl or methylene content per unit mass of toluene was higher than that of cellulose, DA, or CS. It may be that used-$I_{(10)}$-m-CF adsorbed trace amounts of toluene and slightly enhanced its adsorption peak at 2995−2800 cm^{-1}.

CF and modified CF are porous materials rich in capillaries,[37] where the inner surface area is much greater than the outer surface area. Pollutants of toluene and Cu(II) were mainly adsorbed on the inner surface (i.e., the wall of the capillary) and affected the WIT of modified CF, while they hardly affected the UWOCA. Therefore, WIT increased with the time of the experiments, the capillary force of driving water through m-CF decreased, and the *F* value also decreased. Even so, the values of *E* and UWOCA were almost unchanged.

3.4. Adsorption−Desorption Cu(II) Performances of m-CF. The results of the studies mentioned in Section 3.3 showed that m-CF had a certain ability of simultaneous removal of Cu(II) and oil from oily wastewater. On continuous feeding of the oily wastewater, within 120 s (that is, the total time of seven consecutive feeds of oily wastewater) the Cu(II) removal rate decreased from 89 to 67%, and less than 38% in the tenth second. Thus, the following questions were mentioned: (1) Can the removal rate of Cu(II) be increased by changing the operating conditions? (2) Can m-CF regenerate quickly and recover the ability of Cu(II) adsorption? For these reasons, the Cu(II) static adsorption and dynamic desorption experiments of m-CF were carried out, as shown in Figure 8.

The static adsorption experiment of m-CF was carried out with artificial wastewater containing 50 mg·L^{-1} Cu(II) (i.e., Cu(II)−water). Fifty milliliters of wastewater and about 0.40 ± 0.08 g of the m-CF sample were added to a 250 mL conical flask at a constant shaking for 6 h, and then the liquid phase was taken for further analysis. The artificial wastewater containing Cu(II) was prepared with $CuCl_2$ and deionized

https://doi.org/10.1021/acsomega.2c03298
ACS Omega 2022, 7, 30184−30196

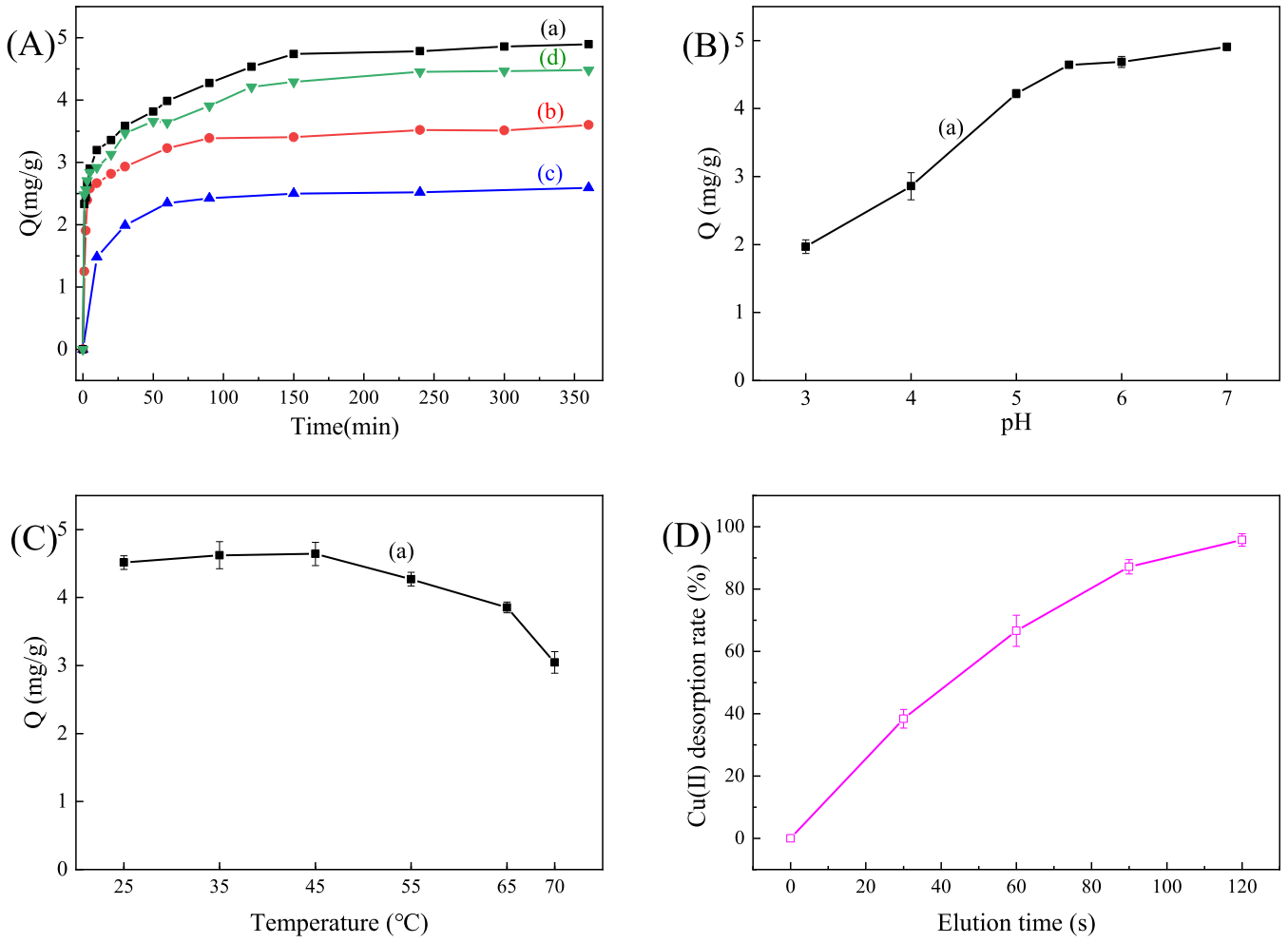

Figure 8. Cu(II) static adsorption experiments (A–C), Cu(II) dynamic desorption experiment of the used-$I_{(10)}$-m-CF (D). (a–c) Treatment of Cu(II)–water by m-CF, CF-PDA, and CF, respectively, (d) treatment of Cu(II)–water–dissolved oil by m-CF.

water, and the initial pH of the wastewater was adjusted using 0.1 mol·L^{-1} NaOH or HCl. The adsorption capacity of Cu(II) is calculated by eq (4). used-$I_{(10)}$-m-CF was fixed on the sand-core apparatus, and the desorption experiment was leached with the HCl solution of 0.1 mol·L^{-1} at 20 mL·min^{-1}. The desorption rate (named D) of Cu(II) is calculated according to eq (10).

$$D = \frac{C_1 V_2}{M_{Cu(II)}} \times 100\% \quad (10)$$

where D is the desorption rate (%) of Cu(II), C_1 and V_2 are the concentration of Cu(II) in the desorption solution (mg·L^{-1}) and the volume of desorption solution (L), and $M_{Cu(II)}$ is the initial Cu(II) content on used-$I_{(10)}$-m-CF (mg).

It can be seen from Figure 8A that the Cu(II) equilibrium adsorption capacities of CF, CF-PDA, and m-CF were 2.59, 3.60, and 4.90 mg·g^{-1}, respectively. Compared with CF, the Cu(II) adsorption capacity of CF-PDA and m-CF increased by 28.1 and 47.1%, respectively. The above results showed that DA and CS loaded with heavy-metal adsorption functional groups (such as $-NH_2$ and $-OH$, etc.) could improve the modified CF adsorption capacity.[9,38] As shown in Figure 8A(a), the adsorption capacity of Cu(II) could reach 50% of the equilibrium adsorption capacity of m-CF within 1 min, indicating that m-CF can remove Cu(II) from wastewater in a short time. Figure 8B,C shows that the effects of pH and temperature on the adsorption of Cu(II) by m-CF were consistent with the results of other studies with CS as the main heavy-metal adsorption composition.[12,39] As the pH increased, the adsorption capacity of Cu(II) decreased slowly,[12,40] and the adsorption capacity decreased with increasing temperature.[41,42] Figure 8A,C shows that the equilibrium adsorption capacity of m-CF was about 4.90 mg·g^{-1} under the experimental conditions of pH 5.6 and Cu(II) concentration of 50 mg·L^{-1}. The literature showed that $-OH$ and $-NH_2$ have a strong binding ability to heavy-metal ions, and $-NH_2$ is the main heavy-metal adsorption site under the condition of weak acid.[9,12,39] Sahebjamee et al.[42] prepared the CS/PVA/PEI membrane for Cu(II) removal, for which the equilibrium adsorption capacity of Cu(II) was 125 mg·g^{-1} under the conditions of 25 °C, pH 6, and Cu(II) concentration of 30 mg·L^{-1}. It was possible that there was either a small amount of PDA and CS on the modified CF or the density of the exposing adsorption groups of the heavy metal was low. The Cu(II) adsorption capacity of m-CF was less than that of other adsorbents based on CS modification, resulting in the low removal rate of the simultaneous removal of Cu(II) from wastewater separation.

Figure 8D shows that when the m-CF containing 11.0 mg·g^{-1} Cu(II) (i.e., used-$I_{(10)}$-m-CF, see Figure 6D) was leached with the HCl solution of 0.1 mol·L^{-1} at 20 mL·min^{-1}, the

https://doi.org/10.1021/acsomega.2c03298
ACS Omega 2022, 7, 30184–30196

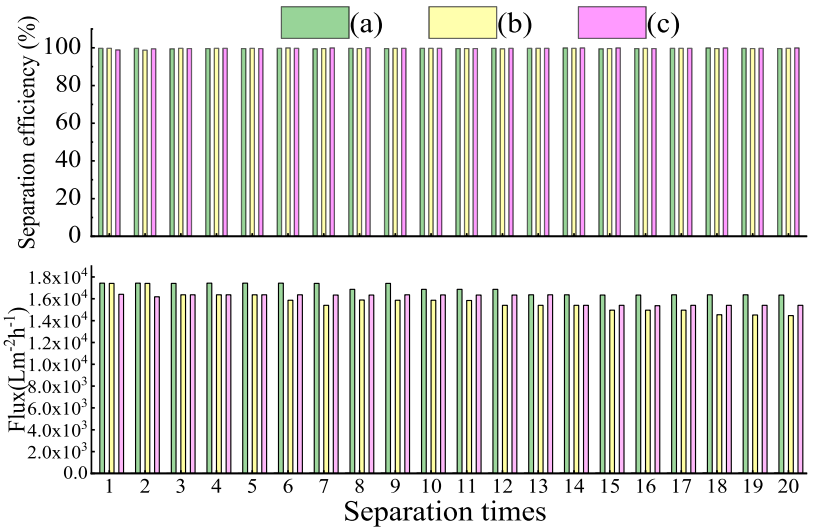

Figure 9. Effect of Cu(II) on the oil−water separation of m-CF at room temperature: (a) treatment of oil−water and (b) Cu(II)−oil−water by m-CF, and (c) treatment of oil−water by $Cu_{(4.90\ mg/g)}$-m-CF.

desorption rate of Cu(II) was more than 95% within 120 s. According to Figures 6D and 8D, we therefore considered that when using multiple oil−water separation devices in parallel, one of the devices simultaneously carried out oil−water separation and adsorption of Cu(II), while another performed the regeneration process, which could be contributing to the simultaneous removal of oil and Cu(II) by m-CF. However, in order to make m-CF suitable for practical application in industry, it is necessary to improve the membrane preparation and desorption processes to increase the adsorption capacity and desorption rate.

3.5. Effect of Cu(II) on Oil−Water Separation. In order to investigate the effect of Cu(II) on the oil−water separation performance, experiments similar to the ones described above in Section 3.3, were carried out with oily wastewater (i.e., oil−water system, 30 mL of toluene, and 70 mL of deionized water) and Cu(II)-containing oily wastewater (i.e., Cu(II)−oil−water system) using m-CF. To make it clear that the m-CF adsorption of Cu(II) (which contained 4.90 $mg{\cdot}g^{-1}$ Cu(II) and was named $Cu_{(4.90\ mg/g)}$-m-CF) was carried out on an oil−water system, see Figure 9.

Figure 9 shows the m-CF-treated Cu(II)−oil−water and oil−water system, respectively. The F values of the first experiment were both 17 400 $L{\cdot}m^{-2}{\cdot}h^{-1}$. But the F value of Cu(II)−oil−water was 14 500 $L{\cdot}m^{-2}{\cdot}h^{-1}$ at the 20th treatment, which decreased by 16.7%, and the F value of oil−water was 16 400 $L{\cdot}m^{-2}{\cdot}h^{-1}$, which only decreased by 5.7%. Obviously, the Cu(II) in wastewater had negatively affected the F value of m-CF.

Figure 9 shows that the F value of $Cu_{(4.90\ mg/g)}$-m-CF was 16 400 $L{\cdot}m^{-2}{\cdot}h^{-1}$ for the first time, which decreased by 6.1% at the 20th treatment. However, the decrease rate of the F value of $Cu_{(4.90\ mg/g)}$-m-CF was much smaller than that of m-CF-treated Cu(II)−oil−water (16.7%). In addition, the Cu(II) contents of the samples treated with oil−water by $Cu_{(4.90\ mg/g)}$-m-CF and Cu(II)−oil−water treated by m-CF for 20 times were analyzed, which were 4.20 and 13.8 $mg{\cdot}g^{-1}$, respectively. The above phenomena showed that the increase of the content of Cu(II) in m-CF will lead to a significant decrease in F value.

It can be seen from Figure 9 that Cu(II) had no influence on the E value, which was more than 98%.

3.6. Effect of Dissolved Oil on the Adsorption of Cu(II). In this study, the effect of trace amounts of dissolved oil in water on Cu(II) removal was studied. Taking 200 mL of deionized water and 30 mL of toluene, the mixture was stirred magnetically at room temperature for 24 h and subjected to stratification. Then, the water phase was taken to further prepare the artificial wastewater with Cu(II), which contained 252 $mg{\cdot}L^{-1}$ dissolved toluene (determined with an infrared spectrophotometry oil measuring instrument) and 50 $mg{\cdot}L^{-1}$ Cu(II) (i.e., Cu(II)−water-dissolved oil). Subsequently, an adsorption experiment was carried out. The results are shown in Figure 8A(d); the equilibrium adsorption capacity of m-CF was 4.50 $mg{\cdot}g^{-1}$, which was 8.2% lower than that for the treatment with "Cu(II)-water" wastewater (Figure 8A(a)). The large π bond in the molecule of toluene endowed it with a certain polarity, and it could interact with polar groups (such as $-NH_2$ and $-OH$) on m-CF, which slightly reduced the adsorption capacity of Cu(II).

3.7. Stability of m-CF. In this work, we investigated the wetting behavior and static adsorption of Cu(II) by m-CF after acid, alkali, and salt immersion treatments and after sandpaper abrasion, as shown in Figure 10.

As shown in Figure 10A, the WITs of m-CF, HCl-m-CF, NaOH-m-CF, $NaCl_{(3.5\%)}$-m-CF, $NaCl_{(10\%)}$-m-CF, $NaCl_{(36\%)}$-m-CF, and abrasion-m-CF were 117, 215, 268, 50, 60, 45, and 180 s, respectively, and UWOCAs were 156.1, 154.9, 154.6, 157.6, 156.1, 154.1, and 152.6°, respectively. There results showed that (1) the WIT of m-CF increased after immersing in acid or alkaline solution for 20 days. On the contrary, (2) the WIT of NaCl-m-CF decreased after immersing for 20 days, and (3) after abrasion, the WIT of m-CF increased. Fortunately, (4) the UWOCAs of all samples were still larger than 150°.

From Figure 10B, compared with m-CF, the equilibrium adsorption of Cu(II) by HCl-m-CF, $NaCl_{(36\%)}$-m-CF, NaOH-m-CF, and abrasion-m-CF were all decreased to 4.04, 4.64, 3.18, and 4.36 $mg{\cdot}g^{-1}$, respectively, i.e., the equilibrium adsorption capacity of Cu(II) decreased by 17.6, 5.3, 35.1, and 11.0%, respectively. What was the reason for the decrease of the equilibrium adsorption of Cu(II) on the m-CF? In order to illustrate the effects of m-CF after treatment in harsh

https://doi.org/10.1021/acsomega.2c03298
ACS Omega 2022, 7, 30184−30196

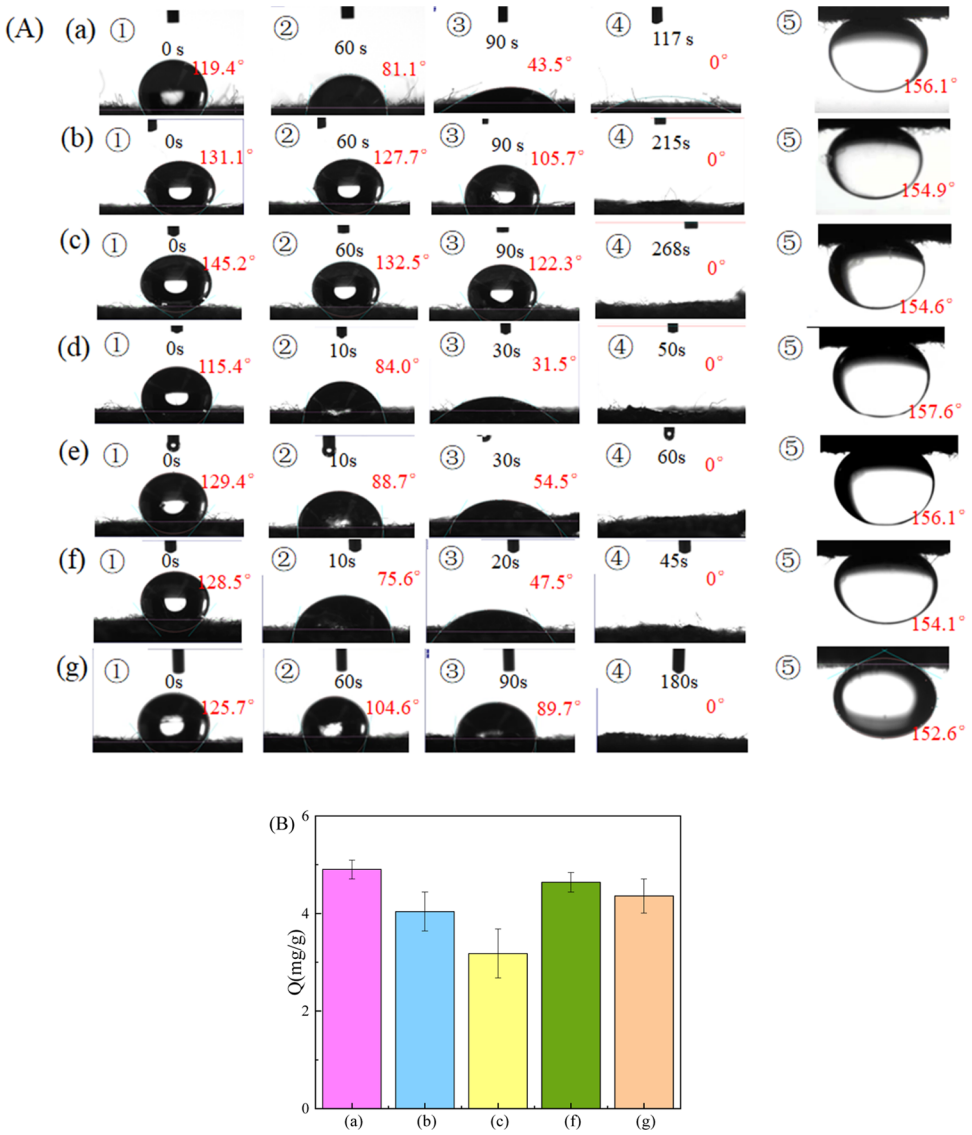

Figure 10. Surface wettability and the Cu(II) adsorption capacity of m-CF after treatment in an artificial environment of acid, alkali, salt, or abrasion (A) and (B), respectively. (a) m-CF, (b) HCl-m-CF, (c) NaOH-m-CF, (d) $NaCl_{(3.5\%)}$-m-CF, (e) $NaCl_{(10\%)}$-m-CF, (f) $NaCl_{(36\%)}$-m-CF, (g) abrasion-m-CF (①–④optical snapshots for dynamic contact processes of the water droplets, ⑤UWOCA).

environment on the wettability and Cu(II) adsorption, SEM and EDS analyses were performed for HCl-m-CF, NaOH-m-CF, $NaCl_{(36\%)}$-m-CF, and abrasion-m-CF, respectively, as shown in Figure 11.

It can be seen from Figure 11a that there were etching holes on the surface of HCl-m-CF, and the content of N element (4.1 wt %) was close to that of m-CF. The H^+ of HCl entered the internal structure of CF, and, adhering to the β-1,4 glycosidic bond of CF, could hydrolyze cellulose, which led to the partial breakage of the cellulose macromolecules and decrease of its polymerization.[43] CS was similar to the cellulose structure (β-1,4 glycosidic bonds), which could be hydrolyzed in acidic aqueous solution, resulting in partial hydrolysis shedding or molecular chain breaking of CS, and forming etching holes. It may also be that the shedding amounts of CS were not much, so that the content of N element did not change obviously. However, the hydrophilicity and the content of polar functional groups ($-NH_3$, $-OH$) chelating with Cu(II) were decreased, resulting in decrease of the equilibrium adsorption of Cu(II).

As shown in Figure 11b, compared with m-CF, the surface roughness of NaOH-m-CF and the content of N element (3.3 wt %) decreased obviously. The loss of PDA deposited on m-CF and the CS adhered on PDA were attributed to the dissolution of PDA by NaOH;[44] thus, the roughness, the content of N element, and the hydrophilicity of the NaOH-m-CF decreased. What's worse, the equilibrium adsorption capacity of Cu(II) was greatly reduced.

From Figure 11c, it can be seen that the surface of $NaCl_{(36\%)}$-m-CF was still rough, the content of N was 4.3 wt %, and there were Na and Cl elements, which may be because NaCl did not dissolve or decompose PDA and CS on m-CF, so that the morphology of NaCl-m-CF was similar to that of m-CF. Additionally, it may be that Na^+ and Cl^- adsorbed on the surface of m-CF and increased the hydrophilicity of the capillary wall,[45] so the WIT of NaCl-m-CF decreased and UWOCA was almost unchanged. However, the residual Na(I) on m-CF competed with Cu(II) for the active site,[40,46] resulting in the decrease of the equilibrium adsorption of Cu(II).

https://doi.org/10.1021/acsomega.2c03298
ACS Omega 2022, 7, 30184–30196

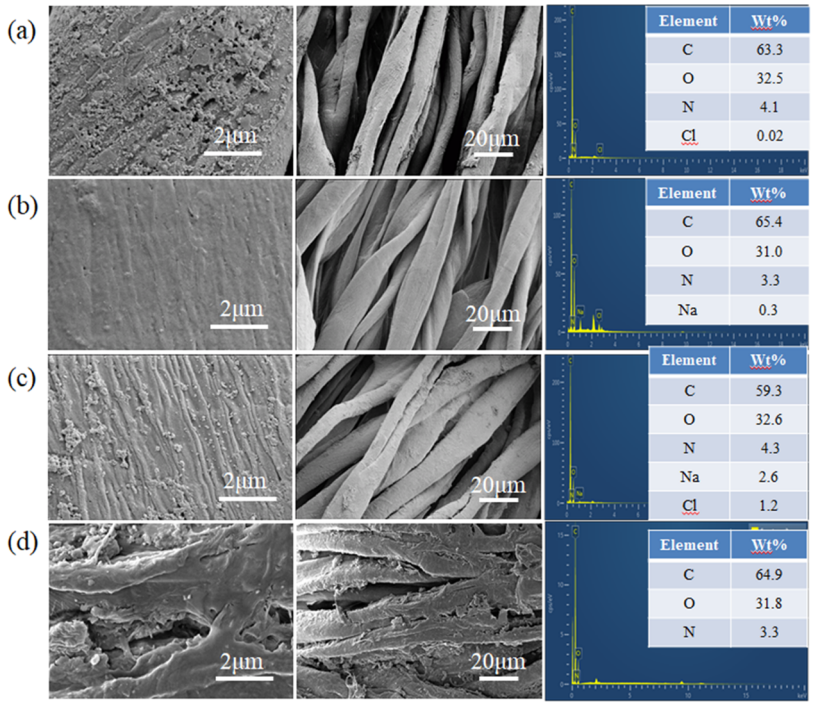

Figure 11. SEM and EDS of m-CF after treatment in an artificial environment of acid, alkali, salt, or abrasion. (a) HCl-m-CF, (b) NaOH-m-CF, (c) $NaCl_{(36\%)}$-m-CF, and (d) abrasion-m-CF.

It can be seen from Figure 11d that abrasion-m-CF was partially worn, resulting in the decrease of N content (3.3 wt %), and indicating that parts of PDA and CS were lost, compared with m-CF, causing the WIT to be increased. It was possible that m-CF immersed in acid, alkali, or salt solution, which had a uniform effect on the inner and outer surfaces of the porous materials. In contrast, the abrasion treatment had a great influence on the outer surface of the porous m-CF and the pores changed. Immersing in acid, alkali, or salt solution changed the WIT of m-CF but UWOCA was almost unchanged, while abrasion treatment changed both WIT and UWOCA (UWOCA decreased, but was still larger than 150°).

In a word, although the *F* value of the oil−water separation of m-CF decreased to some extent under the condition of strong acid or strong alkali or abrasion, as well as the removal ability of Cu(II), its *E* value remained almost unchanged. It showed that m-CF still had good oil−water separation ability under harsh environments (strong acid, strong alkali, high salt and scouring, etc.).

4. CONCLUSIONS

Superhydrophilic and underwater superoleophobic cotton fabric (i.e., m-CF) was prepared using DA and CS, whereby m-CF simultaneously removed the oil and Cu(II) from oily wastewater under gravity, and the oil−water separation efficiency, the water flux, and removal rate of Cu(II) were more than 99%, 17 400 $L{\cdot}m^{-2}{\cdot}h^{-1}$, and 89%, respectively. The oil−water separation efficiency was not affected during the continuous treatment of oily wastewater containing Cu(II), while the water flux of m-CF decreased slowly. Besides, in about 120 s, the Cu(II) removal rate decreased to 67%. The reason we proposed for the decrease of water flux was that both the dissolved oil and Cu(II) on the m-CF and, in turn, trace amounts of dissolved toluene in the water had a slight effect on the removal of Cu(II).

After immersing in strong acid, strong alkali, and high salt solution of m-CF for 20 days at room temperature, and abrasion with 500# sandpaper, the equilibrium adsorption capacity of Cu(II) decreased by 17.6, 35.1, 5.3, and 11.0%, respectively. Although the water droplet infiltration time was prolonged by different degrees (except for the case of high salt), the UWOCAs were still in superoleophobic state. In terms of oil−water separation, m-CF had good acid resistance, alkali resistance, salt resistance, and wear resistance.

The m-CF on which Cu(II) was adsorbed was leached with 0.1 $mol{\cdot}L^{-1}$ HCl solution at 20 $mL{\cdot}min^{-1}$, and the desorption rate within 120 s was more than 95%. The decline rate of the Cu(II) adsorption capacity of m-CF was approximately equal to its desorption rate. Thus, the use of multiple oil−water separation devices in parallel would be conducive to the industrial applications of m-CF.

AUTHOR INFORMATION

Corresponding Authors

Ying Chen − *College of Petrochemical Engineering and Environment, Zhejiang Ocean University, Zhoushan, Zhejiang 316022, P. R. China; United National-Local Engineering Laboratory of Harbor Oil and Gas Storage and Transportation Technology, Zhoushan, Zhejiang 316000, P. R. China; Zhejiang Provincial Key Laboratory of Petrochemical Pollution Control, Zhoushan, Zhejiang 316022, P. R. China*; Email: chenying9468@zjou.edu.cn

Yong Chen − *College of Petrochemical Engineering and Environment, Zhejiang Ocean University, Zhoushan, Zhejiang 316022, P. R. China*; Email: chenyong@zjou.edu.cn

Authors

Xiaohong Li − *College of Petrochemical Engineering and Environment, Zhejiang Ocean University, Zhoushan,*

https://doi.org/10.1021/acsomega.2c03298
ACS Omega 2022, 7, 30184−30196

Zhejiang 316022, P. R. China; orcid.org/0000-0002-8771-0480

Dong Chen − *College of Petrochemical Engineering and Environment, Zhejiang Ocean University, Zhoushan, Zhejiang 316022, P. R. China*

Quan Wang − *College of Petrochemical Engineering and Environment, Zhejiang Ocean University, Zhoushan, Zhejiang 316022, P. R. China*

Yan Wang − *College of Petrochemical Engineering and Environment, Zhejiang Ocean University, Zhoushan, Zhejiang 316022, P. R. China*

Complete contact information is available at: https://pubs.acs.org/10.1021/acsomega.2c03298

Author Contributions

The manuscript was written through the contributions of all authors. All authors have given approval to the final version of the manuscript.

Notes

The authors declare no competing financial interest.

■ ACKNOWLEDGMENTS

This work was supported by the Dinghai District of Zhoushan science and technology project (2021C31002), and the Science and Technology Project of the Bureau of Science and Technology of Zhoushan (2017C41019 and 2019C21028).

■ REFERENCES

(1) Baig, U.; Faizan, M.; Waheed, A. A review on super-wettable porous membranes and materials based on bio-polymeric chitosan for oil-water separation. *Adv. Colloids Interface Sci.* **2022**, *303*, No. 102635.

(2) Hu, G.; Mohammadiun, S.; Gharahbagh, A. A.; Li, J.; Hewage, K.; Sadiq, R. Selection of oil spill response method in Arctic offshore waters: A fuzzy decision tree based framework. *Mar. Pollut. Bull.* **2020**, *161*, No. 111705.

(3) Li, K.; Chen, W.; Wu, W.; Pan, Z.; Liang, Z.; Gan, J. Facile fabrication of superhydrophilic/underwater superoleophobic polyvinyl acetate/sodium silicate composite coating for the effective water/oil separation and the study on the anti-fouling property, durability and separation mechanism. *Prog. Org. Coat.* **2021**, *150*, No. 105979.

(4) Guo, H.; Yang, J.; Xu, T.; Zhao, W.; Zhang, J.; Zhu, Y.; Wen, C.; Li, Q.; Sui, X.; Zhang, L. A robust cotton textile-based material for high-flux oil−water separation. *ACS Appl. Mater. Interface* **2019**, *11*, 13704−13713.

(5) Zhang, Z.; Yu, D.; Xu, X.; Li, H.; Mao, T.; Zheng, C.; Huang, J.; Yang, H.; Niu, Z.; Wu, X. A polypropylene melt-blown strategy for the facile and efficient membrane separation of oil−water mixtures. *Chin. J. Chem. Eng.* **2021**, *29*, 383−390.

(6) Liang, B.; Zhang, G.; Zhong, Z.; Sato, T.; Hozumi, A.; Su, Z. Substrate-independent polyzwitterionic coating for oil/water separation membranes. *Chem. Eng. J.* **2019**, *362*, 126−135.

(7) Qu, M.; Liu, Q.; Liu, L.; Yang, C.; Yuan, S.; Shi, F.; Peng, L.; Xiong, S.; He, J. A superwettable functionalized-fabric with pH-sensitivity for controlled oil/water, organic solvents separation, and selective oil collection from water-rich system. *Sep. Purif. Technol.* **2021**, *254*, No. 117665.

(8) Yu, H.; Wu, M.; Duan, G.; Gong, X. One-step fabrication of eco-friendly superhydrophobic fabrics for high-efficiency oil/water separation and oil spill cleanup. *Nanoscale* **2022**, *14*, 1296−1309.

(9) Nikiforova, T. E.; Kozlov, V. A.; Telegin, F. Y. Chemisorption of copper ions in aqueous acidic solutions by modified chitosan. *Mat. Sci. Eng.* **2021**, *263*, No. 114778.

(10) Peng, W.; Li, H.; Liu, Y.; Song, S. A review on heavy metal ions adsorption from water by graphene oxide and its composites. *J. Mol. Liq.* **2017**, *230*, 496−504.

(11) Jiang, Y.; Cai, W.; Tu, W.; Zhu, M. Facile cross-link method to synthesize magnetic Fe3O4@SiO2−Chitosan with high adsorption capacity toward hexavalent chromium. *J. Chem. Eng. Data* **2019**, *64*, 226−233.

(12) He, W.; Yu, Q.; Wang, N.; Ouyang, X. Efficient adsorption of Cu(II) from aqueous solutions by acid-resistant and recyclable ethylenediamine tetraacetic acid-grafted polyvinyl alcohol/chitosan beads. *J. Mol. Liq.* **2020**, *316*, No. 113856.

(13) Sheth, Y.; Dharaskar, S.; Khalid, M.; Sonawane, S. An environment friendly approach for heavy metal removal from industrial wastewater using chitosan based biosorbent: A review. *Sustainable Energy. Technol. Assess.* **2021**, *43*, No. 100951.

(14) Wang, Y.; Wang, B.; Wang, Q.; Di, J.; Miao, S.; Yu, J. Amino-functionalized porous nanofibrous membranes for simultaneous removal of oil and heavy-metal ions from wastewater. *ACS Appl. Mater. Interfaces* **2019**, *11*, 1672−1679.

(15) Wang, H.; Wang, Z.; Yue, R.; Gao, F.; Ren, R.; Wei, J.; Wang, X.; Kong, Z. Rapid preparation of adsorbent based on mussel inspired chemistry and simultaneous removal of heavy metal ions in water. *Chem. Eng. J.* **2020**, *383*, No. 123107.

(16) Tang, Y.; Li, Y.; Zhang, Y.; Mu, C.; Zhou, J.; Zhang, W.; Shi, B. Nonswelling silica−poly (acrylic acid) composite for efficient and simultaneous removal of cationic dye, heavy metal, and surfactant-stabilized emulsion from wastewater. *Ind. Eng. Chem. Res.* **2020**, *59*, 3383−3393.

(17) Zhai, H.; Qu, R.; Li, X.; Liu, Y.; Zhao, S.; Wei, Y.; Feng, L. A Dually Charged Membrane for Seawater Utilization: Combining Marine Pollution Remediation and Desalination by Simultaneous Removal of Polluted Dispersed Oil, Surfactants, and Ions. *ACS Appl. Mater. Interfaces* **2021**, *13*, 48171−48178.

(18) Li, H.; Mu, P.; Li, J.; Wang, Q. Inverse desert beetle-like ZIF-8/PAN composite nanofibrous membrane for highly efficient separation of oil-in-water emulsions. *J. Mater. Chem. A.* **2021**, *9*, 4167−4175.

(19) Wu, M.; Shi, G.; Liu, W.; Long, Y.; Mu, P.; Li, J. A Universal Strategy for the Preparation of Dual Superlyophobic Surfaces in Oil−Water Systems. *ACS Appl. Mater. Interfaces* **2021**, *13*, 14759−14767.

(20) Zhong, Q.; Shi, G.; Sun, Q.; Mu, P.; Li, J. Robust PVA-GO-TiO2 composite membrane for efficient separation oil-in-water emulsions with stable high flux. *J. Membr. Sci.* **2021**, *640*, No. 119836.

(21) Yan, X.; Zhu, X.; Ruan, Y.; Xing, T.; Chen, G.; Zhou, C. Biomimetic, dopamine-modified superhydrophobic cotton fabric for oil−water separation. *Cellulose* **2020**, *27*, 7873−7885.

(22) Shao, Z.; Lu, J.; Ding, J.; Fan, F.; Sun, X.; Li, P.; Fang, Y.; Hu, Q. Novel green chitosan-pectin gel beads for the removal of Cu(II), Cd(II), Hg(II) and Pb(II) from aqueous solution. *Int. J. Biol. Macromol.* **2021**, *176*, 217−225.

(23) Sabourian, V.; Ebrahimi, A.; Naseri, F.; Irani, M.; Rahimi, A. Fabrication of chitosan/silica nanofibrous adsorbent functionalized with amine groups for the removal of Ni(II), Cu(II) and Pb(II) from aqueous solutions: Batch and column studies. *RSC Adv.* **2016**, *6*, 40354−40365.

(24) Cheng, D.; Zhang, Y.; Liu, Y.; Bai, X.; Ran, J.; Bi, S.; Deng, Z.; Tang, X.; Wu, J.; Cai, G.; Wang, X. Mussel-inspired synthesis of filter cotton-based AgNPs for oil/water separation, antibacterial and catalytic application. *Mater. Today Commun.* **2020**, *25*, No. 101467.

(25) Krishnamoorthi, R.; Anbazhagan, R.; Tsai, H. C.; Wang, C.; Lai, J. Biodegradable, superwettable caffeic acid/chitosan polymer coated cotton fibers for the simultaneous removal of oils, dyes, and metal ions from water. *Chem. Eng. J.* **2022**, *427*, No. 131920.

(26) Li, J.-J.; Zhou, Y.; Luo, Z. Mussel-inspired V-shaped copolymer coating for intelligent oil/water separation. *Chem. Eng. J.* **2017**, *322*, 693−701.

(27) Zhang, G.; Li, Y.; Gao, A.; Zhang, Q.; Cui, J.; Zhao, S.; Zhan, X.; Yan, Y. Bio-inspired underwater superoleophobic PVDF membranes for highly-efficient simultaneous removal of insoluble

emulsified oils and soluble anionic dyes. *Chem. Eng. J.* **2019**, *369*, 576−587.
(28) Zhao, S.; Tao, Z.; Chen, L.; Han, M.; Zhao, B.; Tian, X.; Wang, L.; Meng, F. An antifouling catechol/chitosan-modified polyvinylidene fluoride membrane for sustainable oil-in-water emulsions separation. *Front. Environ. Sci. Eng.* **2021**, *15*, 1−11.
(29) Wang, Y.; Zhang, Y.; Hou, C.; Liu, M. Mussel-inspired synthesis of magnetic polydopamine−chitosan nanoparticles as biosorbent for dyes and metals removal. *J. Taiwan Inst. Chem. Eng.* **2016**, *61*, 292−298.
(30) Wang, M.; Peng, M.; Zhu, J.; Li, Y.; Zeng, J. Mussel-inspired chitosan modified superhydrophilic and underwater superoleophobic cotton fabric for efficient oil/water separation. *Carbohydr. Polym.* **2020**, *244*, No. 116449.
(31) Tian, L.; Li, W.; Ye, H.; Zhu, L.; Chen, H.; Liu, H. Environmentally benign development of superhydrophilic and underwater superoleophobic mesh for effective oil/water separation. *Surf. Coat. Technol.* **2019**, *377*, No. 124892.
(32) Zhou, X.; Zhang, Z.; Xu, X.; Guo, F.; Zhu, X.; Men, X.; Ge, B. Robust and durable superhydrophobic cotton fabrics for oil/water separation. *ACS Appl. Mater. Interfaces* **2013**, *5*, 7208−7214.
(33) Xiao, Q.; Wang, B.; Huang, Y. Preparation and study of stable fluorine-free superhydrophobicity of cotton fibers. *J. Appl. Polym. Sci.* **2021**, *138*, 50556.
(34) Shang, Q.; Cheng, J.; Liu, C.; Hu, L.; Bo, C.; Hu, Y.; Yang, X.; Ren, X.; Zhou, Y.; Lei, W. Fabrication of sustainable and durable biopolybenzoxazine based superhydrophobic cotton fabric for efficient oil/water separation. *Prog. Org. Coat.* **2021**, *158*, No. 106343.
(35) Bahadoran Baghbadorani, N.; Behzad, T.; Etesami, N.; Heidarian, P. Removal of Cu2+ ions by cellulose nanofibers-assisted starch-g-poly (acrylic acid) superadsorbent hydrogels. *Composites, Part B* **2019**, *176*, No. 107084.
(36) Mu'azu, N. D.; Bukhari, A.; Munef, K. Effect of montmorillonite content in natural Saudi Arabian clay on its adsorptive performance for single aqueous uptake of Cu(II) and Ni(II). *J. King Saud Univ., Sci.* **2020**, *32*, 412−422.
(37) Liu, Z.; Fang, K.; Gao, H.; Liu, X.; Zhang, J. Effect of cotton fabric pretreatment on drop spreading and colour performance of reactive dye inks. *Color. Technol.* **2016**, *132*, 407−413.
(38) Zhang, L.; Zeng, Y.; Cheng, Z. Removal of heavy metal ions using chitosan and modified chitosan: A review. *J. Mol. Liq.* **2016**, *214*, 175−191.
(39) Chen, W.; Tang, Q.; Liu, Z.; Luo, F.; Liao, Y.; Zhao, S.; Zhang, K.; Cheng, L.; Ma, D. Fabricating a novel chitosan-based adsorbent with multifunctional synergistic effect for Cu(II) removal: Maleic anhydride as a connecting bridge. *Chem. Eng. Res. Des.* **2020**, *163*, 21−35.
(40) Sun, X.-F.; Hao, Y.; Cao, Y.; Zeng, Q. Superadsorbent hydrogel based on lignin and montmorillonite for Cu(II) ions removal from aqueous solution. *Int. J. Biol. Macromol.* **2019**, *127*, 511−519.
(41) Hu, C.; Zhu, P.; Cai, M.; Hu, H.; Fu, Q. Comparative adsorption of Pb(II), Cu(II) and Cd(II) on chitosan saturated montmorillonite: Kinetic, thermodynamic and equilibrium studies. *Appl. Clay Sci.* **2017**, *143*, 320−326.
(42) Sahebjamee, N.; Soltanieh, M.; Mousavi, S. M.; Heydarinasab, A. Preparation and characterization of porous chitosan−based membrane with enhanced copper ion adsorption performance. *React. Funct. Polym.* **2020**, *154*, No. 104681.
(43) Liu, W.; Liu, S.; Liu, T.; Liu, T.; Zhang, J.; Liu, H. Eco-friendly post-consumer cotton waste recycling for regenerated cellulose fibers. *Carbohydr. Polym.* **2019**, *206*, 141−148.
(44) Kuang, X.-H.; Guan, J.; Tang, R.; Chen, G. Surface functionalization of polyamide fiber via dopamine polymerization. *Mater. Res. Express* **2017**, *4*, No. 095302.
(45) Vatanparast, H.; Shahabi, F.; Bahramian, A.; Javadi, A.; Miller, R. The role of electrostatic repulsion on increasing surface activity of anionic surfactants in the presence of hydrophilic silica nanoparticles. *Sci. Rep.* **2018**, *8*, No. 7251.
(46) Abu-Danso, E.; Peräniemi, S.; Leiviskä, T.; Bhatnagar, A. Synthesis of S-ligand tethered cellulose nanofibers for efficient removal of Pb(II) and Cd(II) ions from synthetic and industrial wastewater. *Environ. Pollut.* **2018**, *242*, 1988−1997.

https://doi.org/10.1021/acsomega.2c03298
ACS Omega 2022, 7, 30184−30196